

Charm particle production in hadronic collisions

C. Avila[†], J. Magnin[‡], L.M. Mendoza-Navas[†]

[†] *Departamento de Física, Universidad de los Andes*

A.A. 4976, Santafé de Bogotá, Colombia

[‡] *Centro Brasileiro de Pesquisas Físicas*

Rua Dr. Xavier Sigaud 150, Urca, CEP 22290-180, Rio de Janeiro, Brazil

February 8, 2020

Abstract

We study charm particle production in hadron-hadron collisions. After calculate perturbatively the charm quark differential cross section, we study the hadronization mechanisms. We show that the recombination mechanism is of fundamental importance to understand the large x_F behaviour of the charm particle differential cross sections as well as the well measured particle antiparticle production asymmetries. It is explicitly shown that the recombination mechanism, oposite to the fragmentation one, break the factorization in charm particle production. Our model is compared to experimental data on charmed hadron production in πN interactions.

1 Introduction

Heavy quark production in hadronic collisions is one of the most interesting testing grounds of Quantum Chromodinamics. The fusion reactions $g\ g \rightarrow Q\ \bar{Q}$ and $q\ \bar{q} \rightarrow Q\ \bar{Q}$ processes are expected to be dominant in heavy quark, Q , production. Actually, experimental data seems to reasonably agree with perturbative QCD (pQCD) calculations which today are available up to Next to Leading Order (NLO) [1].

Once a heavy quark is produced, it has to hadronize to produce the observed final state. On this respect, it was expected that factorization theorem be valid and hadronization proceeded through the fragmentation mechanism. Thus, heavy hadron production can be separated into the perturbatively calculable hard scattering and gluon dynamics from the non-perturbative bound state dynamics contained in the process independent hadron structure, expresed through the corresponding parton distribution functions (PDF), $q(x, Q^2)$ and $g(x, Q^2)$, and the jet fragmentation functions, $D_{h/Q}(z, Q^2)$. Literally speaking, the factorization assumption predicts strict independence of the heavy quark hadronization from the production process. Thus, no flavor correlation should exist between initial and final states.

However, there exist copious experimental information on charm hadron production which contradicts the above hypothesis. In fact, there was observed an excess in the charm hadron production at large values of x_F ($\sim 2p_l/\sqrt{2}$) and a correlation between the leading charm hadrons with the projectile quantum numbers. This suggest the presence of other mechanisms of hadronization which must be operative at large values of x_F and low p_T^2 , as long as fragmentation of the charm quark should not produce either flavor correlations between initial and final states, neither charm hadrons with large x_F . In particular, flavor correlation suggest hadronization mechanisms by which projectile spectators produced at small p_T^2 recombine with charm quarks produced either perturbatively in the hard QCD process, or charm quarks, though perhaps of a non-perturbative nature, already present in the structure of the beam particles.

From a theoretical point of view, several model have been proposed to account for the enhancement of heavy hadron production at large x_F and flavor correlations. Among them we can mention the model of Ref [2], in which a charm quark produced perturbatively recombines with the debris of the projectile, the intrinsic charm model [3], in which a particular Fock state of the projectile containing charm quarks breaks in the collision giving thus the desired flavor correlation between initial and final particles, recombination type models [4] in which charm quarks already present in the projectile structure recombine with light quarks, and models based in the Dual Parton Model and Dual Topological Unitarization [5] in which both, the heavy quark production and hadronization, are treated on a non-perturbative basis.

All the above models have been more or less successful in reproducing the main features of charm hadron production, with possibly the only exception of the intrin-

sic charm model [3], which seems to be excluded [6] by recent experimental data on charmed baryon production in $\pi^- N$ interactions by the E791 [7] and SELEX [8] Collaborations. However, it is important to remark that, although some models are able to reproduce experimental data on production asymmetries, they cannot reproduce simultaneously data on production asymmetries and differential cross sections. This is the case of the intrinsic charm model, as noted in Ref. [6]. This fact indicates that in order to make a meaningful comparison among models and experimental data, both, the differential cross section and the production asymmetry have to be taken into account. As a matter of facts, we have two of three quantities which are, in principle, independent, namely, the differential cross sections of both, particle and antiparticle, or one of the cross sections and the corresponding asymmetry.

In what follows we will analyse the main features of perturbative charm production in hadron-hadron collisions followed by the study of possible hadronization mechanisms. Later, we will compare model results with available experimental data. The last section will be devoted to conclusions.

2 Brief review of perturbative charm production

In the parton model, charm quarks are produced *via* the interaction of partons in the initial hadrons. Thus, the differential cross section as a function of x_F is given by [9]

$$\frac{d\sigma_{c(\bar{c})}}{dx_F} = \frac{1}{2} \sqrt{s} \int H_{ab}(x_a, x_b, \mu_F^2, \mu_R^2) \frac{1}{E} dp_T^2 dy, \quad (1)$$

where H_{ab} is a function which contain information on the structure of the colliding hadrons a, b , and on the hard QCD process which produces the charm quarks. At LO, the function H_{ab} reads

$$\begin{aligned} H_{ab}(x_a, x_b, \mu_F^2, \mu_R^2) = & \Sigma_i \left(q_i^a(x_a, \mu_F^2) \bar{q}_i^b(x_b, \mu_F^2) \right. \\ & + \bar{q}_i^a(x_a, \mu_F^2) q_i^b(x_b, \mu_F^2) \left. \right) \frac{d\hat{\sigma}}{d\hat{t}} |_{q\bar{q}} (\hat{s}, m_c, \mu_R^2) \\ & + g_i^a(x_a, \mu_F^2) g_i^b(x_b, \mu_F^2) \frac{d\hat{\sigma}}{d\hat{t}} |_{gg} (\hat{s}, m_c, \mu_R^2), \end{aligned} \quad (2)$$

with x_a and x_b being the parton momentum fractions, $q(x, \mu_F^2)$ and $g(x, \mu_F^2)$ the quark and gluon momentum distributions in the colliding particles, $\hat{s} = x_a x_b s$ the c.m. energy of the partonic system and μ_F and μ_R the factorization and the renormalization scales. In eq. (1), p_T^2 is the squared transverse momentum of the produced c -quark and y is the rapidity of the \bar{c} quark and E the energy of the produced c -quark. The sum in eq. (2) runs over $i = u, \bar{u}, d, \bar{d}, s, \bar{s}$.

The elementary cross-sections $\frac{d\hat{\sigma}}{d\hat{t}} |_{q\bar{q}}$ and $\frac{d\hat{\sigma}}{d\hat{t}} |_{gg}$ at LO are given by [9, 10].

$$\frac{d\hat{\sigma}}{d\hat{t}} |_{q\bar{q}} = \frac{\pi \alpha_s^2(\mu_R^2)}{9 \hat{m}_c^4} \frac{\cosh(\Delta y) + m_c^2/\hat{m}_c^2}{[1 + \cosh(\Delta y)]^3} \quad (3)$$

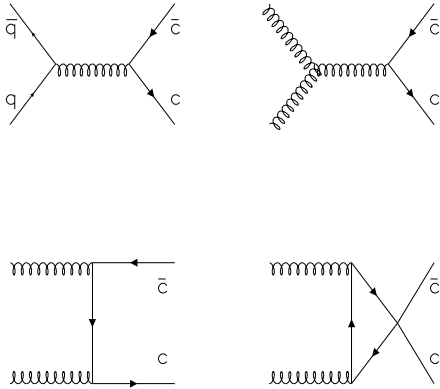


Figure 1: Feynman diagrams for the elementary cross sections entering in eqs. (3) and (4) at LO.

$$\frac{d\hat{\sigma}}{d\hat{t}}|_{gg} = \frac{\pi\alpha_s^2(\mu_R^2)}{96\hat{m}_c^4} \frac{8\cosh(\Delta y) - 1}{[1 + \cosh(\Delta y)]^3} \left[\cosh(\Delta y) + \frac{2m_c^2}{\hat{m}_c^2} + \frac{2m_c^4}{\hat{m}_c^4} \right], \quad (4)$$

where Δy is the rapidity gap between the produced c and \bar{c} quarks and $\hat{m}_c^2 = m_c^2 + p_T^2$. The Feynman diagrams involved in the calculation of eqs. (3) and (4) are shown in Fig. 1.

As shown in eqs. (3-4), at LO the only dependence on μ_R in the elementary cross sections is in $\alpha_s^2(\mu_R^2)$. At this order, the value of the renormalization scale is fixed by the requirement that the propagators in diagrams of Fig. 1 be off-shell by a quantity of at least m_c^2 . So, it is usual to take $\mu_R^2 \sim m_c^2$.

Regarding the factorization scale μ_F , it is the scale at which the initial hadrons see one another in the collision. Then, it fixes the quark and gluon content in the initial hadrons which has to be used in calculations and, hence, its value is of fundamental importance. To illustrate this point, let us imagine that we fix μ_F to some value of the order of the heavy quark mass, as it is usually done. Then, charm has to be considered as forming part of the structure of the initial hadrons, and consequently, more diagrams have to be considered in the LO expression of the differential cross section. The difficulties introduced by doing this has to do with the so called flavor excitation diagrams (see Fig. 2) and has been discussed many times in the literature (see e.g. [1, 10]). Instead of this, in Ref. [1] has been shown that flavor excitation diagrams can be treated consistently because they are a subdiagram of the NLO expressions for the elementary cross sections, avoiding in this way the problems associated with

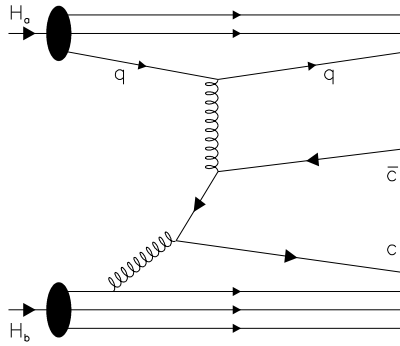


Figure 2: A NLO diagram including a typical flavor excitation subdiagram.

their t -channel pole. However, this implies that the factorization scale has to be fixed to some value $\mu_R < m_c$.

On the other hand, the treatment of flavor excitation diagrams open the discussion about what to do with the charm quark which does not interact with partons in the other hadron. In fact, the momentum distribution of this quark must be the momentum distribution of a charm quark in the sea of the hadrons, since it does not exchange momentum with other partons. The problem here is how to consider this quark in the hadronization part of the reaction. This problem will be discussed in the next section in connection with the recombination of the remnants of the initial hadrons.

It is also known that NLO and LO calculations only differ by a k -factor of the order of 2–3, meaning that calculations can be done consistently at LO and then multiplied by the corresponding k -factor. NLO calculations also show a $c - \bar{c}$ asymmetry [1], which is too small to produce any effect after hadronization.

3 Hadronization mechanisms

There are basically two different models to treat hadronization of the heavy quarks produced in the collision. These are the recombination mechanism and string fragmentation. We will discuss them separately within this section. However, there is a basic requirement for hadronization which is common for any hadronization mechanism. It is that quarks which will form an hadron must be in a color singlet state in

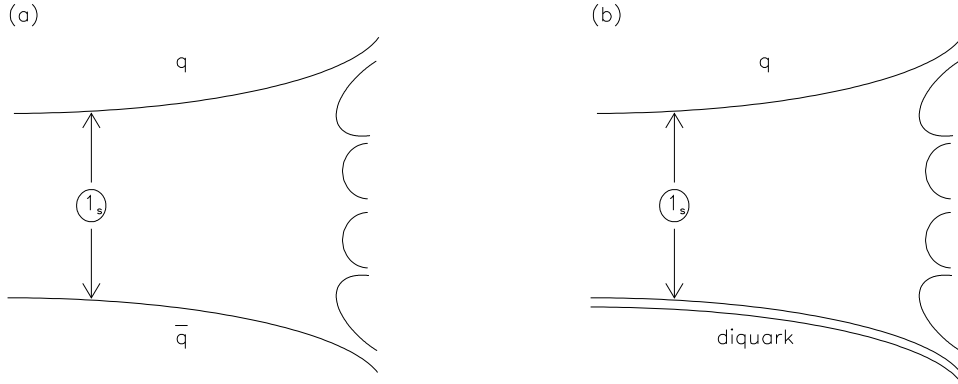


Figure 3: Allowed color string configurations: mesonic string (a) and baryonic string (b).

order to form a colorless hadron. This requirement, which will drive the hadronization of quarks to any hadron state, is not more than a manifestation of confinement in QCD. On the other hand, hadronization of the charm quark is driven by the dynamics of the color string fragmentation mechanism, which limits the kind of processes leading to the production of charm hadrons in the final state. As it is well known, color strings can only be formed from a quark-antiquark or from a quark-diquark pair in a color singlet configuration in order to obtain a purely hadronic final state (see Fig. 3). Furthermore, recombination can be considered as a special case of color string fragmentation which occur when a *short* color string with the quantum numbers of a hadron is formed in the same region of the space.

It is interesting to note that the $q - \bar{q}$ string, which we will name as *mesonic* string, has baryon number zero which is preserved in the final hadronic state. Then, a mesonic string will produce predominantly mesons plus eventual baryon-antibaryon pairs in the final state. Conversely, the $q - \text{diquark}$ string (baryon number one) will produce at least a baryon plus a number of mesons in the final state. It is easy to see that other color string configurations will leave at least a *free* quark in the final state, then they are impossible to occur based in the confinement principle. On the other hand, the requirement that the initial quark configuration, which gives rise to the color string, be in a color singlet state is needed in order to obtain a colorless hadronic final state, as can be easily deduced by drawing the color flux lines for a typical color string configuration.

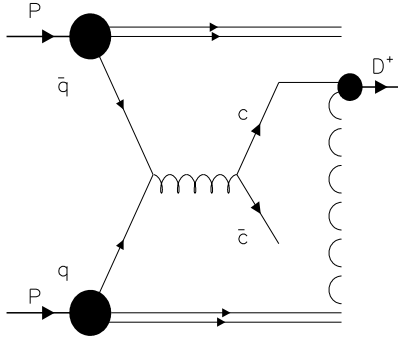


Figure 4: Typical configuration leading to D^+ production in $p - p$ interactions by color string fragmentation.

3.1 String fragmentation

A typical quark configuration leading to color string fragmentation is shown in Fig. 4.

Formation of color strings among the charm quarks and the remnants of the colliding hadrons would give rise to the production of open charm, i.e. D mesons and eventually charm baryons.

This kind of contribution to hadronization is modelled by the convolution of the c -quark differential cross section with a Peterson Fragmentation Function, $D_{H/c}$, [11],

$$\begin{aligned}
 \frac{d\sigma_H}{dx_F} &= \int \frac{dz}{z} \frac{d\sigma_{c(\bar{c})}}{dx} D_{H/c}(z) \\
 z &= \frac{x_F}{x} \\
 D_{H/c}(z) &= \frac{N}{z \left(1 - \frac{1}{z} - \frac{\epsilon}{1-z}\right)^2}, \tag{5}
 \end{aligned}$$

where $\epsilon \sim m_q/m_Q$ and $d\sigma_{c(\bar{c})}/dx$ is given in eq. (1).

3.2 Recombination

A typical quark configuration leading to recombination is shown in Fig. 5.

The contribution of the recombination mechanism can be estimated by means

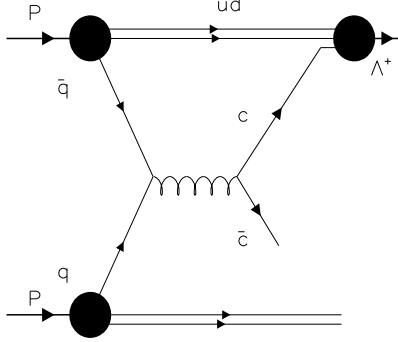


Figure 5: Typical configuration leading to Λ_c^+ production in $p - p$ interactions by recombination.

of [2]

$$\frac{d\sigma}{dx_F} = \frac{\sqrt{s}}{2} \int x_v z^* \frac{d\sigma^*}{dx_v dz} R(x_v, z, x_F) \frac{dx_v}{x_v} \frac{dz}{z}, \quad (6)$$

where $R(x, z, x_F)$ is the recombination function, for which we shall use [12]

$$R(x, z, x_F) = \beta \frac{x}{x_F^2} \frac{z}{z} \delta \left(1 - \frac{x+z}{x_F} \right), \quad (7)$$

with β a normalization parameter which has to be fixed from experimental data. In eq. (6), $z^* = 2E_c/\sqrt{2}$ and

$$\begin{aligned} \frac{d\sigma^*}{dx_v dz} &= q_v(x_v, \mu_F^2) \frac{d\hat{\sigma}}{dx_v dz}, \\ \frac{d\hat{\sigma}}{dx_v dz} &= q^v(x_v, \mu_F^2) \int_0^W dp_T^2 \int_{z_+/1-z_-}^{1-x_v} \frac{H_{ab}(x_a, x_b, \mu_F^2, \mu_R^2)}{x_a - z_+} dx_a \end{aligned} \quad (8)$$

where H_{ab} is given in eq. (2), x_v is the fraction of the momentum of the hadron a carried by the spectator quark q_v^a , $z^* = 2E_c/\sqrt{s}$, $z = 2p_{z,c}/\sqrt{s}$, $z_{\pm} = \frac{1}{2}(z^* \pm z)$, $x_b = x_a z_- / (x_a - z_+)$ and

$$\begin{aligned} E_c &= \sqrt{m_T^2 + p_{z,c}^2} \\ W &= \frac{s(1-x_v-z)(1-x_v)(1+z)}{(2-x_v)^2} - m_c^2. \end{aligned} \quad (9)$$

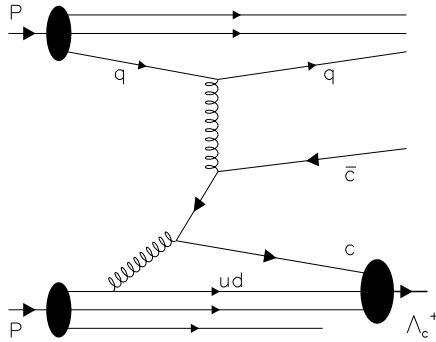


Figure 6: Typical configuration leading to Λ_c^+ production in $p - p$ interactions by spectator recombination.

In eq. (8), q_v^a represent either a quark or a diquark momentum distribution, depending if the final hadron is a meson or a baryon. Note that, as the quark or diquark are part of the structure of one of the colliding hadrons, this introduces a flavor correlation among initial and final hadrons, as observed in experimental data.

Another possibility is that the *spectator* charm quark in Fig. 2 recombines with the debris of its own hadron. It is clear from the figure that the momentum distribution of the charm and the anticharm are different. What one encounters when calculating charm hadroproduction at NLO is the differential cross section for the heavy quark which interacts through a gluon with partons in the other hadron (the anticharm in Fig. 2). The momentum distribution of the *spectator* heavy quark can be found by looking at the corresponding quark distribution function in the hadron at the Q^2 scale to which the process is being calculated. To calculate then the differential cross section for the recombination of the spectator quark with the debris of the own hadron, the recombination model à lá Das-Hwa [12] is called for (see Fig. 6).

In this case, the production of leading mesons at low p_T can be described [12] by means of

$$\frac{d\sigma^{rec}}{dx_F} = \beta \int_0^{x_F} \frac{dx_1}{x_1} \frac{dx_2}{x_2} F_2(x_1, x_2) R_2(x_1, x_2, x_F), \quad (10)$$

where x_i , $i = 1, 2$, is the momentum fraction of the i^{th} quark, $F_2(x_1, x_2)$ is the two-quark distribution function in the hadron and $R_2(x_1, x_2, x_F)$ is the two-quark recombination function and β is a normalization constant which must be fixed by comparison to experimental data. A version of the model to consider baryon produc-

tion has been developed by Ranft [13]. Along this work we will use

$$F_i(x_1, \dots, x_i) = \prod_{j=1}^i f_j(x_j, \mu_F^2) \left(1 - \sum_{j=1}^i x_j\right)^\gamma$$

$$i = 2, 3, \quad (11)$$

with $\gamma = 1$ for $i = 2$ and $\gamma = -0.1$ for $i = 3$ [4].

For the recombination function we shall use its simplest version given by

$$R_i(x_1, \dots, x_i, x_f) = \frac{\prod_{j=1}^i x_j}{x_f^{i-1}} \delta \left(1 - \frac{\sum_{j=1}^i x_j}{x_F}\right).$$

$$i = 2, 3 \quad (12)$$

4 Modeling and comparison to experimental data

So far, there exist in the literature experimental data on D meson production from experiments WA82 [14] and WA92 [15]. In these experiments, neutral and charged D mesons are produced in π^- *Nucleus* interactions at beam energies of the order of 350 GeV/c. In order to compare theoretical calculation against experimental data we used

$$\frac{d\sigma}{dx_F} = a \frac{d\sigma}{dx_F}^{frag} + b \frac{d\sigma}{dx_F}^{recI} + c \frac{d\sigma}{dx_F}^{recII}, \quad (13)$$

where the first term in the right hand side of eq. (13) accounts for D meson production through fragmentation and its expression is given in eqs. (5); the second term represents the D meson production by the recombination of the perturbatively generated charm quark with spectator quarks from the beam particles as given in eq. (6); and finally we included the third term representing the production of D mesons via the recombination of spectator charm quarks in NLO diagrams with the debris of the beam particles and whose expression is given in eq. (10). a , b , and c are coefficients which were fixed by fitting the experimental data.

In Fig. 7 we display the results of our fit to experimental data on D^-/D^+ and D^0/\bar{D}^0 production in 350 GeV/c beam energy π^- – *Nucleus* interactions by the WA92 Collaboration [15]. As can be seen in the figures, the model describes quite well the experimental data for both charged and neutral D mesons. Our fit also shows that charm quark fragmentation and recombination of the charm quark produced in the hard QCD process with the debris of the initial beam particles is enough to describe the data. As expected, the contribution of the recombination of the spectator charm quark remaining from NLO diagrams with valence quarks in the initial particles is negligible.

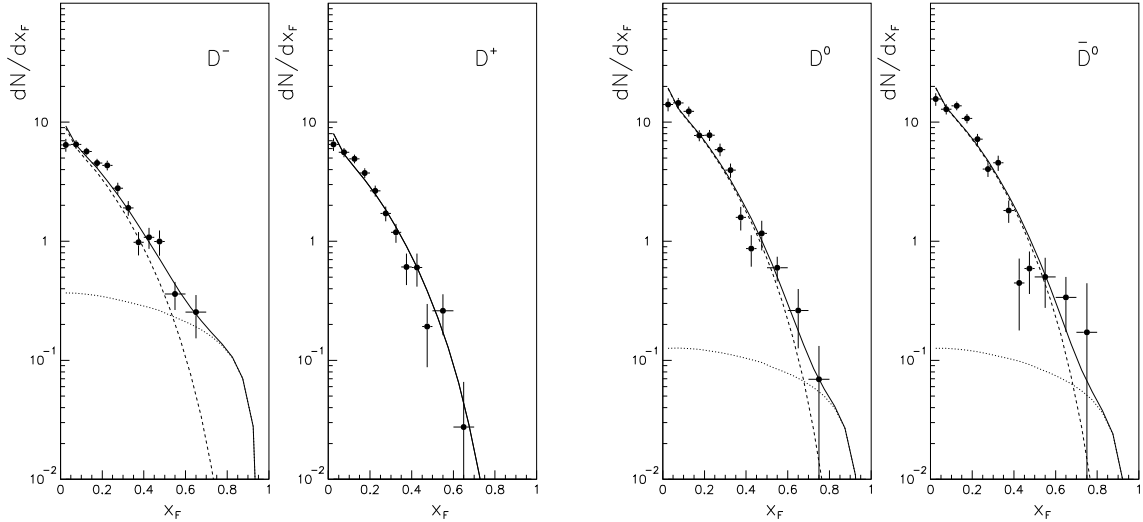


Figure 7: Charged and neutral D production in π^- *Nucleus* interactions at 350 GeV/ c beam energy. Data from the WA92 Collaboration [15]. Full line: our model as in eq. (13). Dashed line: contribution from fragmentation. Point line: contribution from recombination.

In Fig. 8 we display the results of our fit to experimental data on D^-/D^+ production and asymmetry by the WA82 Collaboration [14]. Note that the WA82 Collaboration measured the particle distribution as a function of x_F for D^- and D^+ and the production asymmetry as a function of x_F . As from these three sets of data, only two are independent, we fitted the D^- and D^+ particle distributions and obtained from these fits the production asymmetry.

Once again, as evidenced in the figures, the result of the fit describes well the experimental data on both, production and production asymmetry. We do not included any contribution coming from the recombination of the spectator charm quark in then initial pion from NLO diagrams. We show also the asymmetry as obtained from fits to WA92 [15] data. As can be seen in the figure, both curves are similar and describe well the WA82 data on production asymmetry, giving support to the idea that asymmetries are independent of the collision energy. It has to be noted that, in fits to the WA82 data, a small contribution from the recombination of the hard QCD charm quark with the debris of the initial pion is necessary, oposite to what happens with the WA92 data. This behavior could be due to the high value of the last experimental point, not observed in the WA92 data.

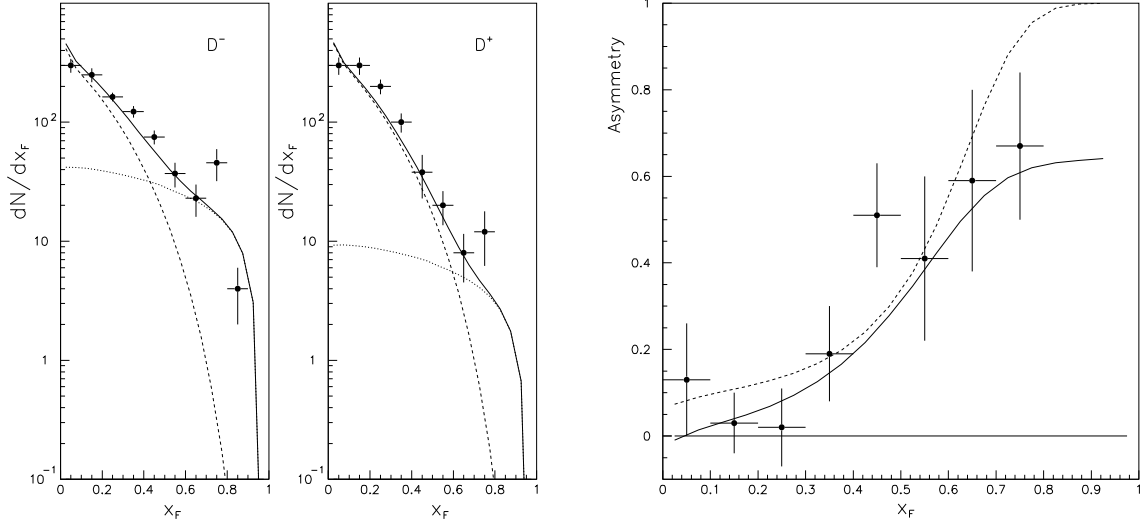


Figure 8: Left: D^- and D^+ production in π^- *Nucleus* interactions at 340 GeV/c beam energy. Data from the WA82 Collaboration [14]. Full line: our model as in eq. (13). Dashed line: contribution from fragmentation. Point line: contribution from recombination. Right: D^-/D^+ production asymmetry. Data from Ref. [14]. Full line: Our calculation (see eq. (14)). Dashed line: Our prediction for the D^-/D^+ asymmetry from fits to D^- and D^+ production by WA92 [15].

The production asymmetry has been calculated as

$$A(x_F) = \frac{dN^L/dx_F - dN^{NL}/dx_F}{dN^L/dx_F + dN^{NL}/dx_F}, \quad (14)$$

where L is for Leading and NL is for Non Leading particles.

In Fig. 9 we show the data and fits to the $D^*(2010)$ production in 500 GeV/c π^- *Nucleus* interactions by the E791 Collaboration [16]. The E791 measured the $D^{*-} + D^{*+}$ particle distribution as a function of x_F as well the D^{*-}/D^{*+} production asymmetry. In order to fit the data with our model of eq. 13, we fitted simultaneously the $D^{*-} + D^{*+}$ particle distribution and the production asymmetry. From the fits, we extracted the individual D^{*-} and D^{*+} particle distributions.

As can be seen in the figure, our curves agree well with the experimental data. Once again, no contribution from spectator charm quark recombination from NLO diagrams was necessary.

Finally, in Fig. 10, we display the data and fit results for Λ_c production and production asymmetry obtained in 600 GeV/c π^- *Nucleus* interactions by the SELEX Collaboration [8]. Here we fitted the Λ_c^+ and Λ_c^- particle distributions and obtained

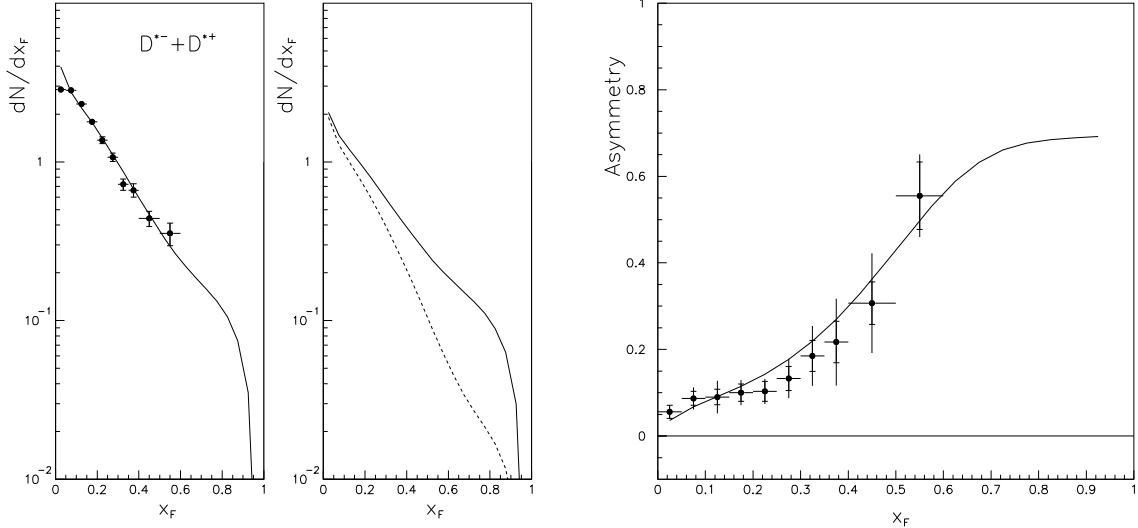


Figure 9: Left: $D^{*-} + D^{*+}$ production in π^- *Nucleus* interactions at 500 GeV/ c beam energy. Data from the E791 Collaboration [14]. Full line: our model as in eq. (13). Middle: Full line: our prediction for D^{*-} production. Dashed line: our prediction for D^{*+} production. Right: D^{*-}/D^{*+} production asymmetry. Data from Ref. [16]. Full line: our fit (see eq. (14)).

the asymmetry from our fit functions. As can be seen in the figures, our theoretical curves agree well with the experimental data.

Regarding the Λ_c^+/Λ_c^- production asymmetry, some comments are in order. Λ_c^- production in π^- *Nucleus* interactions follows from the fragmentation of the perturbatively produced \bar{c} quark and by the recombination of the \bar{c} quark with a $\bar{u}\bar{d}$ diquark in the π^- . In a π^- , the \bar{u} is a valence quark while the \bar{d} is a sea quark. On the other hand, Λ_c^+ production follows from the fragmentation of the perturbatively produced c quark followed by the recombination of the c quark with a ud diquark in the π^- , where the d is a valence quark and the u is a sea quark. However, a \bar{u} quark in the π^- can easily annihilate with a u valence quark in the target particles. As this is not possible for the u and d quarks which form the diquark needed for Λ_c^+ production, Λ_c^- production is suppressed in π^- *Nucleus* interactions, as discussed in Ref. [6]. This is then the origin of the observed asymmetry in the SELEX [8] and E791 [7] data.

5 Conclusions

We have shown that using a simple model based on perturbative QCD for charm quark production and on well known hadronization mechanisms, namely fragmenta-

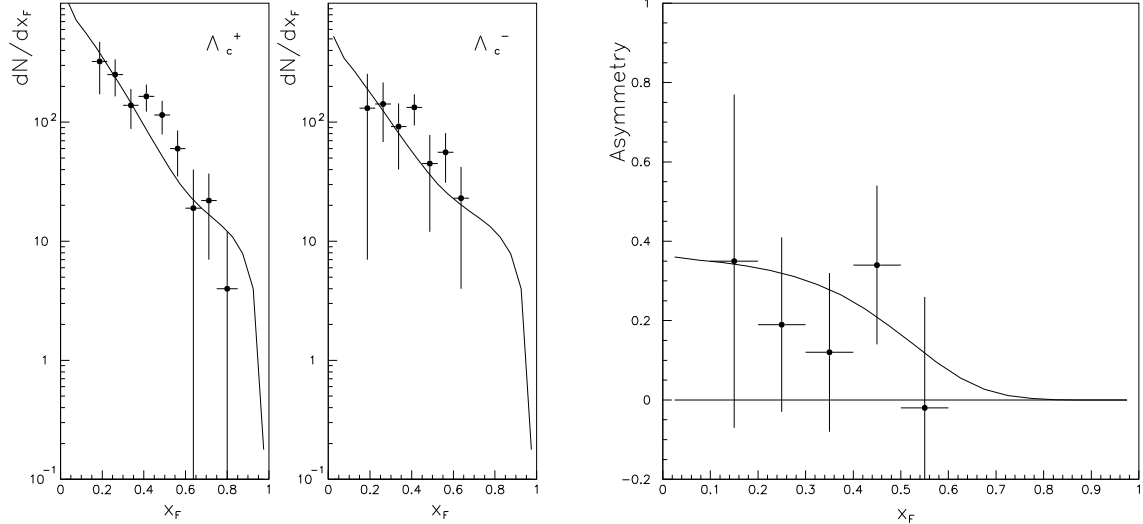


Figure 10: Λ_c^+ (left) and Λ_c^- (middle) production in π^- *Nucleus* interactions at 600 GeV/c beam energy. Data from the SELEX Collaboration [8]. Full line: our model as in eq. (13). Right: Λ_c^+/Λ_c^- production asymmetry. Data from Ref. [8]. Full line: our fit (see eq. (14)).

tion and recombination, the available experimental data on charm hadron production can be well described. The model considers the production of charm hadrons *via* the fragmentation of the perturbatively produced charm quark as well as by the recombination of perturbative charm quarks with the debris of the initial hadrons. These are well known hadronization mechanisms. The idea of describing charm hadron production through the fragmentation and recombination of perturbatively produced charm quarks is not new. It has been discussed by the first time in Ref. [2], but never has been extensively tested against all the available experimental data.

Our analysis has shown that intrinsic charm is not needed in order to describe consistently the experimental data on both charm particle distributions and charm particle production asymmetries. This was evident once SELEX data on Λ_c baryons and antibaryons became available, as noted in Ref. [6].

Parameters in the model of eq. (13) are not particularly meaningful, at least while more precise experimental data be available. They represent the unknowns associated to the fractions of the fragmentation and recombination contributions, but also include the uncertainties coming from the non-perturbative contributions to the hadronization process. It is conceivable that with more abundant and precise experimental data, the behavior of this parameters with respect to the reaction and reaction energy can be fixed, allowing in this way a more predictive power of the model.

In Refs. [4, 6] another model including the recombination of charm quarks with the debris of the initial particles was considered. However, in this model, recombining charm quarks were considered as part of the structure of the initial particles. The fact that both, the model discussed here and the model of Refs. [4, 6], are able to describe well the experimental data is due to the fact that the momentum distribution of perturbatively produced charm quarks is similar to the sea charm quark distribution in hadrons. It is easy to see that this is a consequence of the fact that in both cases the origin of the charm quarks is gluon splitting, then its momentum distributions must be similar.

In addition, we have shown that factorization is broken as long as the structure of the initial colliding particles has to be taken into account in order to describe the hadronization of charm quarks. However, it does not mean that new unknowns are added to the problem. There still exist a consistent way to calculate hadronization within the framework of the recombination model.

Acknowledgments

J. Magnin would like to thank the warm hospitality at the Physics Department, Universidad de los Andes, where part of this work was done. L.M. Mendoza-Navas would like to thank the warm hospitality at CBPF during his stay for the completion of the work. This work was supported by Fundación para la Promoción de la Investigación y la Tecnología del Banco de la República (Colombia) under contract Project #1376.

References

- [1] P. Nason, S. Dawson and R.K. Ellis, Nucl. Phys. **B 327** (1989) 49.
- [2] V.G. Kartvelishvili, A.K. Likhoded and S.R. Slabospitskii, Sov. J. Nucl. Phys. **28** (1978) 678; *ibid.* **33** (1981) 434.
- [3] S.J. Brodsky, P. Hoyer, C. Peterson and N. Sakai, Phys. Lett. **B 93** (1980) 451; S.J. Brodsky, C. Peterson and N. Sakai, Phys. Rev. **D 23** (1981) 2745.
- [4] E. Cuautle, G. Herrera and J. Magnin, Eur. Phys. J. **C 2** (1998) 473; G. Herrera and J. Magnin, Eur. Phys. J. **C 2** (1998) 477; J. dos Anjos, G. Herrera, J. Magnin and F.R.A. Simão, Phys. Rev. **D 56** (1997) 394.
- [5] O.I. Piskunova, hep-ph/0202005 and references therein.
- [6] J.C. Anjos, J. Magnin and G. Herrera, Phys. Lett. **B 523** (2001) 29.
- [7] E.M. Aitala *et al.* (E791 Collaboration), Phys. Lett. **B 495** (2000) 42.

- [8] F.G. Garcia *et al.* (SELEX Collaboration), Phys. Lett. **B 528** (2002) 49.
- [9] J. Babcock, D. Sivers and S. Wolfram, Phys. Rev. **D 18** (1978) 162, R.K. Ellis, Fermilab-Conf-89/168-T (1989), I. Inchiliffe, Lectures at the 1989 SLAC Summer Institute, LBL-28468 (1989).
- [10] B.L. Combridge, Nucl. Phys. **B 151** (1979) 429.
- [11] C. Peterson, D. Schlatter, J. Schmitt and P. Zerwas, Phys. Rev. **D 27** (1983) 105.
- [12] K.P. Das and R.C. Hwa, Phys. Lett. **B68** (1977) 459, Erratum *ibid.* **B73** (1978) 504.
- [13] J. Ranft, Phys. Rev. **D 18** (1978) 1491.
- [14] M. Adamovich *et al.* (WA82 Colaboration), Phys. Lett. **B305** (1993) 402.
- [15] M. Adamovich *et al.* (WA92 Collaboration), Nucl Phys. **B495** (1997) 3.
- [16] E.M. Aitala *et al.* (E791 Collaboration), Phys. Lett. **B539** (2002) 218.